articles

molecular pharmaceutics

The p53 Inhibitor Pifithrin-α Forms a Sparingly Soluble Derivative via Intramolecular Cyclization under Physiological Conditions

Ronald K. Gary* and Derek A. Jensen

Department of Chemistry, University of Nevada, Las Vegas, Nevada 89154

Received July 3, 2005

Abstract: The transcription factor p53 coordinates cell cycle arrest and apoptosis in response to DNA damage. Pifithrin-α (PFT-α) is a small molecule inhibitor of p53 activity that is frequently used in cell culture studies of p53 function. Here we report an investigation of the stability of this compound. PFT-α rapidly converts to a planar tricyclic derivative, with a half-life of 4.2 h under physiological conditions. This spontaneous conversion greatly alters the structural and physicochemical properties of the drug. PFT-α has a pK_a of 9.11 and is an ionic species in physiological medium, whereas the tricyclic derivative has a pK_a of 4.36 and exists as the neutral free base at pH 7. The tricyclic derivative is very hydrophobic, with a log *P* of 4.26. Although PFT-α is generally used at 10−30 μM concentration, the aqueous solubility of its derivative is only 0.2 μM, and it can form a visible precipitate under conditions of typical use. The conversion of PFT-α proceeds via an intramolecular cyclization reaction involving the imine and carbonyl groups. Modification of the carbonyl function creates a stable analogue of PFT-α that remains soluble indefinitely. These results provide a strategy for the rational design of PFT-α analogues that exhibit predictable stability, hydrophobicity, and aqueous solubility.

Keywords: Pifithrin-α; cyclic-PFT; p53; solubility; pK_a; log *P*; HPLC; imine; ketone; cyclization; rational drug design

Introduction

The TP53 gene is often mutated in human cancers. Inactivation of TP53 is estimated to be important in the etiology of at least half of all tumors, making this the most important human tumor suppressor by the criterion of mutation frequency. The gene product p53 serves to coordinate diverse cellular responses to DNA damage, such as cell cycle arrest, upregulation of DNA repair pathways, and apoptosis. p53 is multifunctional and has complex interactions with numerous cell signaling pathways. Much of the function of p53 derives from its role as a transcription factor capable of turning on the expression of cell cycle regulatory proteins such as p21 (Waf1/Cip1) and apoptosis-promoting proteins such as bax.[1] Evidence from chromatin immunoprecipitation studies suggests that the transactivating activity of p53 may control the expression of more than a hundred different genes.[2]

The activity of p53 can be antagonized by endogenous regulatory proteins such as MDM2, and by viral oncoproteins such as human papillomavirus E6. Because p53 has a vital role in opposing carcinogenesis, preserving p53 function is paramount. However, pharmacological antagonists of p53 are very useful in experimental investigations of p53 function and may have therapeutic utility as well. To date, pifithrin-α (PFT-α) and its analogues are the only small molecule

* Corresponding author. Mailing address: Department of Chemistry, Mail Code 4003, University of Nevada, Las Vegas, 4505 Maryland Parkway, Las Vegas, NV 89154. Tel: (702) 895-1687. Fax: (702) 895-4072. E-mail: rogary@ccmail.nevada.edu.

(1) Levine, A. J. p53, the cellular gatekeeper for growth and division. *Cell* **1997**, *88*, 323−331.

(2) Chen, J.; Sadowski, I. Identification of the mismatch repair genes PMS2 and MLH1 as p53 target genes by using serial analysis of binding elements. *Proc. Natl. Acad. Sci. U.S.A.* **2005**, *102*, 4813−4818.

10.1021/mp050055d CCC: $30.25
Published on Web 10/01/2005

antagonists of p53 transcriptional activity known. The compound 2-(2-imino-4,5,6,7-tetrahydrobenzothiazol-3-yl)-1-*p*-tolylethanone, named pifithrin-α as an acronym for p-fifty-three-inhibitor, was discovered as the lone "hit" during a screen of a 10 000 compound chemical library for the ability to inhibit p53-mediated transcription.[3] In this study, it was shown that PFT-α produces dose-dependent inhibition of p53-responsive reporter gene expression in mammalian cells treated with 10−30 μM PFT-α. PFT-α also protects cells from p53-mediated apoptosis in a variety of contexts. The drug increases cell survival after exposure to UV light or DNA-damaging chemotherapeutic agents such as doxorubicin and etoposide. In MCF-7 human tumor cells, PFT-α blocks doxorubicin-induced activation of caspase-3, a key effector protease in the apoptotic signaling cascade.[4] Remarkably, systemically administered PFT-α allows mice to survive a lethal dose of whole body γ radiation.[3]

Numerous therapeutic applications have been envisioned for reversible small molecule p53 inhibitors.[5] It has been proposed that these drugs might someday be used to help ease the side effects of cancer treatment. Many of the undesirable side effects of radiation and chemotherapy, such as anemia, fatigue, immunosuppression, nausea, and hair loss, occur when normal cells are killed by the treatment. To a significant extent, the death of the normal cells under these circumstances is p53-mediated, such that the apoptotic response to DNA damage, rather than the direct lethal effects of the damage per se, are responsible for a sizable portion of the side effects. If it were possible to transiently suppress p53 in normal cells of the intestinal tract or hematopoietic centers during administration of radiation or chemotherapy, great benefit to the patient could result. Chemoprevention of p53-mediated cell death might also be desirable during ischemia and reperfusion or in the treatment of certain neurodegenerative disorders.[6] In a rat model of cerebral injury due to ischemic stroke, PFT-α was found to reduce brain damage by several criteria.[7]

PFT-α has been used extensively in cultured cells for basic research to assess the p53 dependence of various phenomena. Protocols for the use of PFT-α vary considerably. Cells may be treated with the drug for a few hours or for several days. It is not uncommon for cells to be pretreated with PFT-α for up to 24 h and then challenged with a p53-activating stimulus. For inhibition of p53-mediated transcription, PFT-α is most often used at doses of 10−30 μM, although higher concentrations are occasionally tested. In human embryonic kidney cells, 100 μM PFT-α was more effective than 10 or 30 μM doses in inhibiting doxorubicin-induced expression of p21 protein.[8] Nonetheless, PFT-α exhibits much greater potency in certain cell survival assays. Submicromolar concentrations of PFT-α are capable of protecting primary hippocampal neurons and rat neuronal PC12 cells from cell death elicited by topoisomerase poisons.[9,10] The wide range of effective concentrations observed in different assay formats seems surprising, but this subject has not received much discussion. Investigation of the molecular pharmaceutics of this compound could provide insight into its unusual variations in potency.

There is one commercially available analogue of PFT-α, called cyclic-PFT, but it has not been well characterized. With very few exceptions, investigators have relied on PFT-α exclusively for pharmacological inhibition of p53. Cyclic-PFT is the tricyclic imidazobenzothiazole derivative of PFT-α, and it can be synthesized from the parent compound by boiling in ethanol under reflux.[11,12] A recent analysis of PFT-α and novel PFT-α analogues found that this reaction is relatively facile when electron withdrawing substituents are present on the phenyl ring.[13] We observed insoluble precipitate in PFT-α treated cells and established that this

(3) Komarov, P. G.; Komarova, E. A.; Kondratov, R. V.; Christov-Tselkov, K.; Coon, J. S.; Chernov, M. V.; Gudkov, A. V. A chemical inhibitor of p53 that protects mice from the side effects of cancer therapy. *Science* **1999**, *285*, 1733−1737.

(4) Wang, S.; Konorev, E. A.; Kotamraju, S.; Joseph, J.; Kalivendi, S.; Kalyanaraman, B. Doxorubicin induces apoptosis in normal and tumor cells via distinctly different mechanisms: intermediacy of H_2O_2- and p53-dependent pathways. *J. Biol. Chem.* **2004**, *279*, 25535−25543.

(5) Komarova, E. A.; Gudkov, A. V. Chemoprotection from p53-dependent apoptosis: potential clinical applications of the p53 inhibitors. *Biochem. Pharmacol.* **2001**, *62*, 657−667.

(6) Gudkov, A. V.; Komarova, E. A. Prospective therapeutic applications of p53 inhibitors. *Biochem. Biophys. Res. Commun.* **2005**, *331*, 726−736.

(7) Leker, R. R.; Aharonowiz, M.; Greig, N. H.; Ovadia, H. The role of p53-induced apoptosis in cerebral ischemia: effects of the p53 inhibitor pifithrin-α. *Exp. Neurol.* **2004**, *187*, 478−486.

(8) Murphy, P. J.; Galigniana, M. D,; Morishima, Y.; Harrell, J. M.; Kwok, R. P.; Ljungman, M.; Pratt, W. B. Pifithrin-alpha inhibits p53 signaling after interaction of the tumor suppressor protein with hsp90 and its nuclear translocation. *J. Biol. Chem.* **2004**, *279*, 30195−30201.

(9) Culmsee, C.; Zhu, X.; Yu, Q. S.; Chan, S. L.; Camandola, S.; Guo, Z.; Greig, N. H.; Mattson, M. P. A synthetic inhibitor of p53 protects neurons against death induced by ischemic and excitotoxic insults, and amyloid beta-peptide. *J. Neurochem.* **2001**, *77*, 220−228.

(10) Zhu, X.; Yu, Q. S.; Cutler, R. G.; Culmsee, C. W.; Holloway, H. W.; Lahiri, D. K.; Mattson, M. P.; Greig, N. H. Novel p53 inactivators with neuroprotective action: syntheses and pharmacological evaluation of 2-imino-2,3,4,5,6,7-hexahydrobenzothiazole and 2-imino-2,3,4,5,6,7-hexahydrobenzoxazole derivatives. *J. Med. Chem.* **2002**, *45*, 5090−5097.

(11) Singh, A.; Mohan, J.; Pujari, H. K. Heterocyclic systems containing bridgehead nitrogen atom: Part XXV—Synthesis of imidazo-[2,1-*b*]benzothiazoles and quinoxalino[2,3:4′,5′]imidazo[2′,1′-*b*]-benzothiazoles. *Indian J. Chem., Sect. B: Org. Chem. Incl. Med. Chem.* **1976**, *14*, 997−998.

(12) Balse, M. N.; Mahajanshetti, C. S. Condensed tetrahydrobenzothiazoles: Part III—Synthesis of 2-aryl-5,6,7,8-tetrahydroimidazo[2,1-*b*]benzothiazoles and 1,2,3,4-tetrahydrobenzimidazo-[2′,1′-*b*]benzothiazoles and their 4/5 carbethoxy derivatives. *Indian J. Chem., Sect. B: Org. Chem. Incl. Med. Chem.* **1980**, *19*, 263−265.

(13) Pietrancosta, N.; Maina, F.; Dono, R.; Moumen, A.; Garino, C.; Laras, Y.; Burlet, S.; Quelever, G.; Kraus, J. L. Novel cyclized pifithrin-α p53 inactivators: synthesis and biological studies. *Bioorg. Med. Chem. Lett.* **2005**, *15*, 1561−1564.

material was due to the tricyclic derivative. The relationship between the cyclization process and the appearance of the insoluble material was confirmed by synthesizing and characterizing an analogue of PFT-α that is unable to cyclize. It seems an inescapable conclusion that most studies of PFT-α activity have been conducted in the presence of a significant fraction of the tricyclic derivative that has been generated in situ during the course of the experiment. In light of this, we have characterized some of the physicochemical properties of the tricyclic derivative that are of greatest importance in pharmaceutics, and found them to be very different from those of the parent compound. It is possible that the tricyclic derivative may be responsible for some of the activities that have been thought to be attributable to the PFT-α structure.

Materials and Methods

Chemical Synthesis of PFT-α and Its Analogues. PFT-α (compound **1**) HBr was purchased from Sigma-Aldrich (St. Louis, MO) or synthesized as previously described.[10] Briefly, 2-amino-4,5,6,7-tetrahydrobenzothiazole was prepared from cyclohexanone, thiourea, and iodine, then N-alkylated at the thiazole with 2-bromo-4′-methylacetophenone, and purified by recrystallization. Cyclic-PFT (compound **2**) HBr was from Sigma-Aldrich or prepared by cyclization of PFT-α. Compound **3** was synthesized by N-alkylation of 2-amino-4,5,6,7-tetrahydrobenzothiazole with benzyl bromide as previously described.[10]

Documentation of Drug Precipitation during Cell Culture. HFL-1 cells were seeded into 24-well plates in RPMI cell culture medium (Gibco-Invitrogen, Carlsbad, CA) supplemented with 10% fetal bovine serum (FBS; HyClone, Logan, UT) and antibiotics and allowed to attach overnight. Medium was replaced with fresh RPMI, 10% FBS, and antibiotics plus 30 μM PFT-α from DMSO stock and growth continued for 24 h at 37 °C. Phase-contrast images were photographed at 100× magnification on a Nikon TS100 microscope. Larger crystals that formed in RPMI without serum were photographed at 40× magnification.

Gradient HPLC. PFT-α was resolved from its degradation product by reversed-phase HPLC on a C18 column. A Waters 2695 HPLC was used to run a 10 min 40−90% methanol−water gradient at a flow rate of 0.5 mL min^{-1}. Tris-HCl (10 mM) (delivered as 100 mM at 10% of mobile phase volume) was included to maintain the pH at 6.5. The full mobile phase program for each run was 40% MeOH (3 min), 40−90% gradient (10 min), 90% MeOH (3 min), return to 40% (4 min), and reequilibrate at 40% MeOH in preparation for the next injection (4 min). Analyte injection volumes were 10 or 20 μL. HPLC absorbance traces were recorded at 260 nm, and peak areas were integrated using Waters Empower software and expressed in units of μV•s.

Reaction Kinetics. A 10 mM PFT-α stock in DMSO was diluted 1:50 with water to give a 98% H_2O/2% DMSO vehicle and then incubated in a 37 °C bath for 0, 2, 3, 4, 6, or 19 h. The amount of undegraded PFT-α remaining at each time was determined by adding 100 μL of the aqueous sample to 300 μL of isopropyl alcohol and 600 μL of methanol and immediately quantitating by HPLC. The peak area for PFT-α monitored at 260 nm was plotted as a function of time, and the data were fitted to an equation of the form $y = ae^{-bx}$ to determine the half-life. For the DMSO half-life study, time points were collected at 0, 2, 4, 6, 17, and 20 h, and four times as much material was analyzed.

Measurement of pK_a. Solid PFT-α HBr or cyclic-PFT HBr was dissolved in methanol and analyzed by titration of methanol−water cosolvent mixtures at 25 °C, in a total volume of 6−10 mL. The tendency of the neutral species to precipitate limited the concentration of analyte and the percentage of water that could be used in the titrations. Cyclic-PFT was titrated at 0.68−1.2 mM in 50−70% (w/w) methanol, with precipitation occurring during titrations attempted with less than 50% methanol. The neutral species of PFT-α was somewhat more soluble in methanol−water mixtures, so it could be titrated at 1.61−2.53 mM in 45−60% methanol. All titrations were conducted in the presence of 0.1 M KCl. Compounds were titrated with 0.05 or 0.10 M KOH in 0.1 M KCl and 50% (w/w) MeOH, so that changes in ionic strength and methanol concentration were negligible as titrant was added. Solutions were overlaid with argon to minimize the absorption of atmospheric carbon dioxide during titration. To correct for the effects of the methanol cosolvent on pH readings, the calibration procedure of Avdeef et al. was employed.[14] First, the pH electrode (Corning combination electrode 476436) was calibrated with aqueous pH standards. In the methanol−water cosolvents, operational pH readings (the observed values) were converted to p_cH using the four-parameter equation for glass electrode calibration: $pH_{obs} = \alpha + S\ p_cH + j_H[H^+] + j_{OH}[OH^-]$. Values for the electrode standardization parameters α, S, j_H, and j_{OH} for various methanol−water mixtures were obtained from the literature.[14] The four-parameter equation is regarded to be generally applicable to glass electrodes.[15] The applicability of these standardization parameters to the electrode used in this study was established by two criteria. First, acetic acid, a reference analyte characterized previously,[14] was titrated in various methanol−water cosolvent mixtures, and the p_cH values produced using the four-parameter equation were in excellent agreement with the published results (data not shown). Second, application of the four-parameter equation improved the R^2 value for the linear regression on Yasuda−Shedlovsky plots compared to plots based on pH_{obs} for both PFT-α and cyclic-PFT.

The equivalence point, V_e, was taken as the maximum of $d(pH)/dV_b$, the first derivative of the titration plot. The methanol−water p_sK_a values were obtained by calculating

(14) Avdeef, A.; Comer, J. E. A.; Thomson, S. J. pH-metric log *P*. 3. Glass electrode calibration in methanol−water, applied to pK_a determination of water-insoluble substances. *Anal. Chem.* **1993**, *65*, 42−49.

(15) Avdeef, A.; Box, K. J.; Comer, J. E. A.; Gilges, M.; Hadley, M.; Hibbert, C.; Patterson, W.; Tam, K. Y. pH-metric logP. 11. pK_a determination of water-insoluble drugs in organic solvent−water mixtures. *J. Pharm. Biomed. Anal.* **1999**, *20*, 631−641.

the p_cH at one-half V_e for each titration. The aqueous pK_a was determined by extrapolating the plot of $p_sK_a + \log [H_2O]$ versus $1/\epsilon$ according to the Yasuda−Shedlovsky procedure,[16] using values for ϵ, the dielectric constant, that have been tabulated for methanol−water mixtures.[17] The aqueous pK_a was found by subtracting log(55.5) from the *y*-intercept value of $p_sK_a + \log [H_2O]$ at which *x* equals 0.01274, the inverse of the dielectric constant for 100% water. For pure water at 25 °C, $\epsilon = 78.48$,[17] and $[H_2O] = 55.5$ M.

Measurement of log *P*. The logarithm of the octanol−water partition coefficient, log *P*, was measured by isocratic HPLC. Cyclic-PFT and a series of *n*-alkylbenzene standards were analyzed as 10 μL injections by reversed-phase HPLC on a Waters Symmetry C18 column (particle size 3.5 μm, 4.6 mm i.d., 75 mm length). HPLC was conducted at 25 °C with methanol−water mobile phases of varying composition, reported as volume fraction of methanol. In order to measure the partition behavior of the neutral species of cyclic-PFT during log *P* determination, the mobile phase was kept at pH 8.5 by inclusion of Tris-HCl buffer at 10 mM final concentration. Ionization of cyclic-PFT is completely suppressed at this pH. Capacity factor (k') was calculated by $(t_R - t_0)/t_0$. The k' values were extrapolated to zero methanol to obtain k'_w, which was related to log *P* using the standards.

Aqueous Solubility. Standard curves of compound **2** (cyclic-PFT) dissolved in methanol were used to obtain molar extinction coefficients. All measurements were done by absorbance scanning from 350 to 230 nm in a 1 cm path length quartz cuvette on a Varian Cary 50 UV−vis spectrophotometer. The aqueous solubility was measured several times, either in slightly buffered water, containing 2 mM potassium phosphate at pH 7.0, or in standard formulation phosphate-buffered saline (PBS), containing 10 mM potassium phosphate, pH 7.0, with 150 mM NaCl. Ionic strength had no effect on aqueous solubility. The water or PBS also contained 1% MeOH (v/v) final concentration, because the cyclic-PFT was added from a methanol stock. Saturated suspensions were allowed to reach equilibrium by incubating with continuous agitation for 24 h at room temperature (25 °C). Insoluble particulate was removed by filtration through a 0.45 μm GHP acrodisc polypropylene syringe filter (25 mm diameter) with glass fiber prefilter, HPLC-certified for low UV-detectable extractables (Pall Gelman Laboratory, Ann Arbor, MI). Parallel filtrations with water/1% methanol blanks showed the release of low but detectable quantities of UV-absorbing extractables originating from the filter. These were nearly eliminated by discarding the first 3 mL of filtrate from each filter. To correct for the very small quantity of UV-absorbing material that continued to be leached from the precleared filters, absorbance values of blank filtrates were subtracted from those of analyte-containing filtrates. The average corrected absorbance of the filtrate from the saturated aqueous solution of cyclic-PFT was converted to concentration using Beer's law.

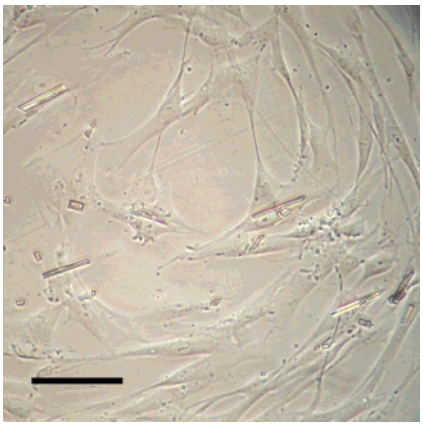

Figure 1. Presence of crystalline material in cell cultures treated with PFT-α. The scale bar indicates 100 μm.

Molecular Modeling. PFT-α and its tricyclic derivative were constructed in the Builder module of InsightII using an O2 Silicon Graphics workstation. Each compound was modeled using the ionic form present at pH 7, i.e., the protonated imine for PFT-α and the neutral free base for the tricyclic derivative. For each structure, energy minimization was performed using the Discover application with the ESFF force field[18] with Steepest Descents followed by Quasi Newton (BFGS) until convergence was reached as defined by RMS gradient less than 0.01 kcal mol^{-1} $Å^{-1}$. For display, the two structures were superimposed at the tetrahydrobenzothiazole rings.

Results

PFT-α Forms an Insoluble Derivative Spontaneously under Physiological Conditions. At concentrations often used to treat cells, PFT-α formed an insoluble precipitate in cell culture medium. Fibroblasts were treated with 30 μM PFT-α in RPMI culture medium with 10% FBS and photographed 24 h later (Figure 1). Crystals were generally clustered near the center of the well. Precipitate was not observed in wells that contained medium without PFT-α. Crystals formed from 30 μM PFT-α in medium containing 10% FBS and in medium with serum omitted, but the abundance of visible precipitate was much greater in the latter, suggesting that serum proteins, probably albumin, suppressed crystal formation. Albumin is a carrier of lipophilic substances. In an experiment done in culture medium without serum, the formation of precipitate was rapid and temperature-dependent (Figure 2). The solubility of a solid compound generally increases with temperature, so the increase in precipitate at elevated temperature indicates that

(16) Avdeef, A. Physicochemical profiling (solubility, permeability and charge state). *Curr. Top. Med. Chem.* **2001**, *1*, 277−351.

(17) Albright, P. S.; Gosting, L. J. Dielectric constants of the methanol−water system from 5 to 55°. *J. Am. Chem. Soc.* **1946**, *68*, 1061−1063.

(18) Shi, S.; Yan, L.; Yang, Y.; Fisher-Shaulsky, J.; Thacher, T. An extensible and systematic force field, ESFF, for molecular modeling of organic, inorganic, and organometallic systems. *J. Comput. Chem.* **2003**, *24*, 1059−1076.

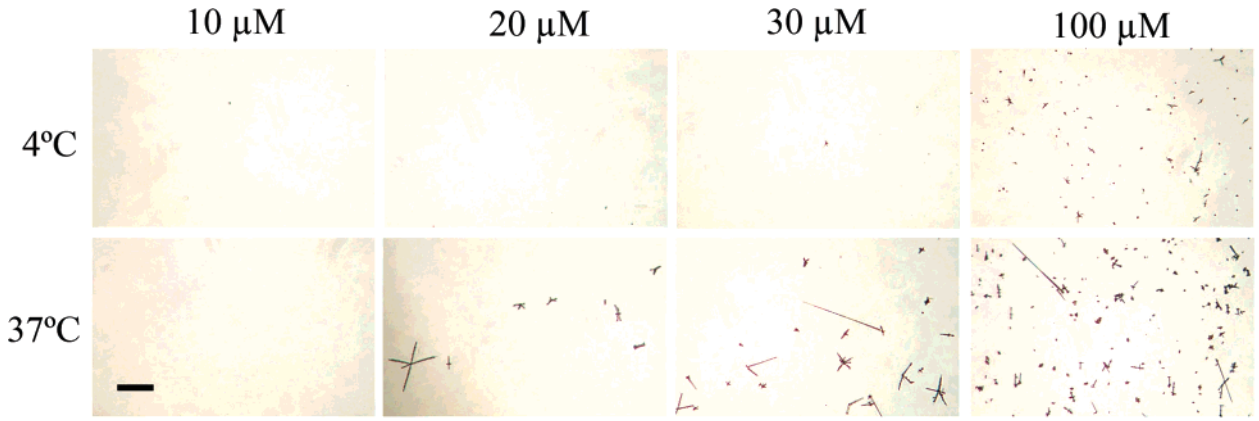

Figure 2. A temperature-dependent process converts PFT-α to an insoluble product. PFT-α at 10, 20, 30, or 100 μM after 8 h in culture medium at 4 or 37 °C. A 100 μm scale bar is shown in the lower left.

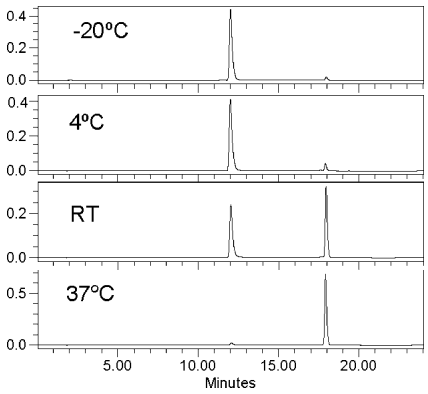

Figure 3. Temperature-dependent degradation of PFT-α, analyzed by HPLC. After 24 h at −20 °C, 4 °C, room temperature, or 37 °C, PFT-α (retention time 12.03 min) formed a product with retention time of 17.96 min.

the compound precipitating is not PFT-α itself, but a product derived from PFT-α by chemical reaction.

A reversed-phase HPLC method was developed to separate PFT-α from its less soluble derivative. When a C18 column was used with methanol/water gradient elution, PFT-α had a retention time of 12.03 min, and its degradation product a retention time of 17.96 min. A methanol solution of PFT-α was incubated for 24 h at −20 °C, 4 °C, room temperature (25 °C), or 37 °C and then analyzed by HPLC (Figure 3). PFT-α spontaneously converted to the product in a temperature-dependent manner. After 24 h at 37 °C, PFT-α was almost completely degraded. Starting with 97% pure PFT-α, the fraction of intact PFT-α remaining after 24 h of incubation was 94% at 4 °C, 53% at room temperature, and only 4% at 37 °C, based on HPLC peak areas.

Identification of the PFT-α Degradation Product. Proton NMR spectra were used to determine the structure of the product formed during temperature-dependent degradation of PFT-α. ^{1}H NMR 500 MHz (DMSO-d_6) for PFT-α: δ 9.49 (s, 2H), 7.95 (d, J = 8.2 Hz, 2H), 7.44 (d, J = 8.1 Hz, 2H), 5.70 (s, 2H), 2.55 (s, 2H), 2.43 (s, 3H), 2.32 (s, 2H), 1.73 (m, 4H). ^{1}H NMR 500 MHz (DMSO-d_6) for degradation product: δ 8.51 (s, 1H), 7.71 (d, J = 8.1 Hz, 2H), 7.32 (d, J = 8.1 Hz, 2H), 2.76 (m, 4H), 2.35 (s, 3H),

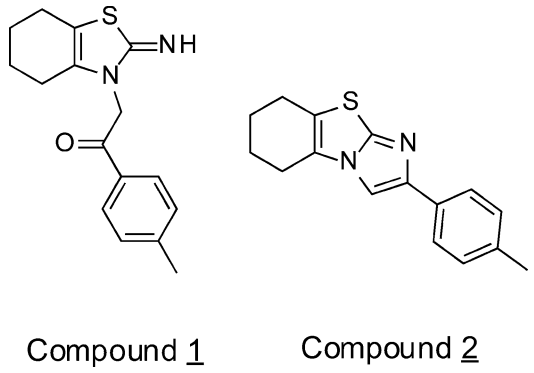

Figure 4. Chemical structures of PFT-α (compound **1**) and its tricyclic derivative (compound **2**).

1.89 (m, 4H). On the basis of the proton NMR, the PFT-α degradation product was determined to be 2-(4-methylphenyl)imidazo[2,1-*b*]-5,6,7,8-tetrahydrobenzothiazole (Figure 4, compound **2**), a compound that is commercially available under the name cyclic-PFT. The NMR data for PFT-α were consistent with previously reported values,[10] with one notable exception. Whereas a single proton with chemical shift 8.85 ppm had previously been noted for the imine peak, we observed that dissolution of solid PFT-α hydrobromide salt directly into anhydrous deuterated DMSO yielded an imine peak with two-proton integration at 9.49 ppm. The presence of two chemically equivalent protons at this position indicates that PFT-α HBr salt was stably protonated at the imine under these conditions. Subsequent experiments described below confirmed that the exocyclic imine of PFT-α is a strong base that can be expected to be stably protonated. A second previous report of PFT-α NMR data[13] differed somewhat from the results reported here, most significantly in the chemical shift of the pair of protons that are α to the ketone of PFT-α (4.70 versus 5.70 ppm reported here). For compound **2**, the peaks corresponding to the imine and the methylene protons α to the ketone were absent, and a new one-proton peak at 8.51 ppm appeared which corresponds to the imidazole ring proton that is unique to this structure. The proton NMR spectrum of compound **2** has been reported once before,[13] but our results differed. For example, the chemical shift values of the two doublet peaks produced by

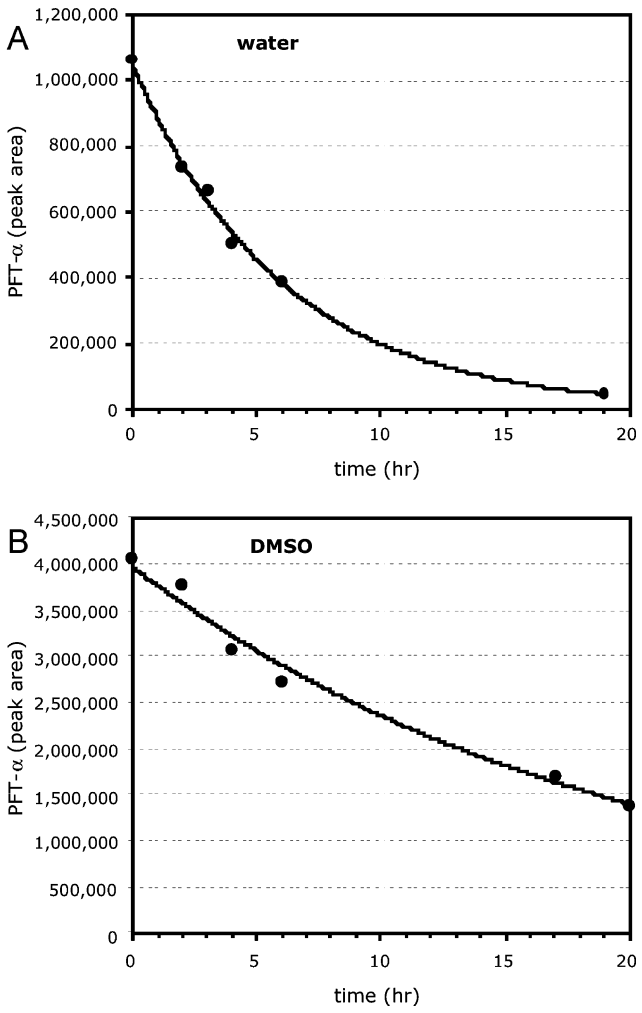

Figure 5. Loss of PFT-α as a function of time in water (panel A) or DMSO (panel B) at 37 °C. Exponential decay curves fit to the data indicated $t_{1/2}$ = 4.2 h (water) and $t_{1/2}$ = 13.3 h (DMSO).

the phenyl ring protons had been reported to be identical in PFT-α and compound **2**, but we observed that each doublet was shifted upfield in compound **2**. In fact, the NMR spectrum of a mixture of PFT-α and its degradation product reveals four well-separated doublets between 7.3 and 8.0 ppm that can be integrated to estimate the purity of the preparation.

Reaction Kinetics. The rate of degradation of PFT-α under physiological conditions was investigated (Figure 5). Stability was also determined in DMSO, which is the usual solvent for making stock solutions of the drug. HPLC was used to measure the amount of PFT-α remaining as a function of incubation time at 37 °C. The data fit a standard exponential decay curve for both water (R^2 = 0.9989) and DMSO (R^2 = 0.9882). In water, the degradation of PFT-α to its tricyclic derivative occurred with a half-life of 4.2 h. PFT-α was appreciably more stable in DMSO, with a half-life of 13.3 h in this solvent.

Characterization of the Tricyclic Derivative: pK_a. In order to better understand the large differences in aqueous solubilities and chromatographic behaviors for PFT-α and its tricyclic derivative, their acid dissociation constants were measured by potentiometric titration and reported as pK_a. The aqueous pK_a could not be measured directly because the unprotonated species of these compounds have limited solubility. Therefore, the titrations were conducted in methanol−water solutions at the highest analyte concentrations permitted by solubility constraints. PFT-α was titrated in 45%, 50%, 55%, and 60% (w/w) MeOH, and cyclic-PFT was titrated in 50%, 55%, 60%, 65%, and 70% (w/w) MeOH. Titrations attempted at lower methanol concentrations ended in precipitation. Titrations in 55% MeOH are shown to illustrate the appearance of the raw data (Figure 6). The inflection indicating the equivalence point (V_e) of the titration was much less distinct for PFT-α, a trend that is typical for base titrations of compounds with pK_a's above 9. The volume of base required to reach the equivalence point was determined by the maximum in the first derivative of the titration plot. This derivative had a single-point maximum for all titrations except PFT-α at 45% and 55% MeOH, which had two-point and three-point plateaus, respectively (see Figure 6, panel B). In these cases, the midpoint of the plateau was taken as the maximum. For each methanol−water mixture, the apparent pK_a (p$_s K_a$) was found by the pH at one-half V_e. Apparent pK_a's based on the observed pH readings are given in Table 1. However, observed pH readings differ from the true proton concentration-based p$_c$H values due to effects of the methanol cosolvent on the potential sensed by the electrode. To adjust for these effects, pH$_{obs}$ values were converted to p$_c$H values according to the four-parameter electrode calibration method described in the Materials and Methods section. The p$_s K_a$ values based on p$_c$H are shown (Table 1) and were used for subsequent analysis.

The acid dissociation behavior of a compound is influenced by the composition of its solvent. For compounds that are bases, the apparent pK_a is expected to decrease as the concentration of methanol in the cosolvent is increased. Interestingly, this relationship was not observed when only the pH$_{obs}$ for PFT-α at 45−50% MeOH was considered, but the rank ordering of these values conformed to the expected pattern after the electrode calibration procedure was employed to obtain p$_c$H values (Table 1).

The Yasuda−Shedlovsky extrapolation was used to infer the aqueous pK_a from the apparent pK_a's observed in the methanol−water mixtures.[16] By describing the methanol−water mixtures in terms of their dielectric constants and their molar water concentrations, a linear relationship can be obtained that allows the apparent pK_a's to be extrapolated to zero methanol. When plotted in this manner, the titration data displayed good linearity, with R^2 = 0.9870 and R^2 = 0.9971 for the linear regressions of PFT-α and cyclic-PFT, respectively (Figure 7). The slopes of the two regression lines were remarkably similar (−124.77 and −128.17). The *y*-axis values of the Yasuda−Shedlovsky plot, which denote the sum p$_s K_a$ + log [H_2O], are tabulated along with the extrapolated value that corresponds to zero methanol (Table 1). The molar concentration of H_2O in pure water is 55.5; therefore log(55.5) was subtracted from the extrapolated

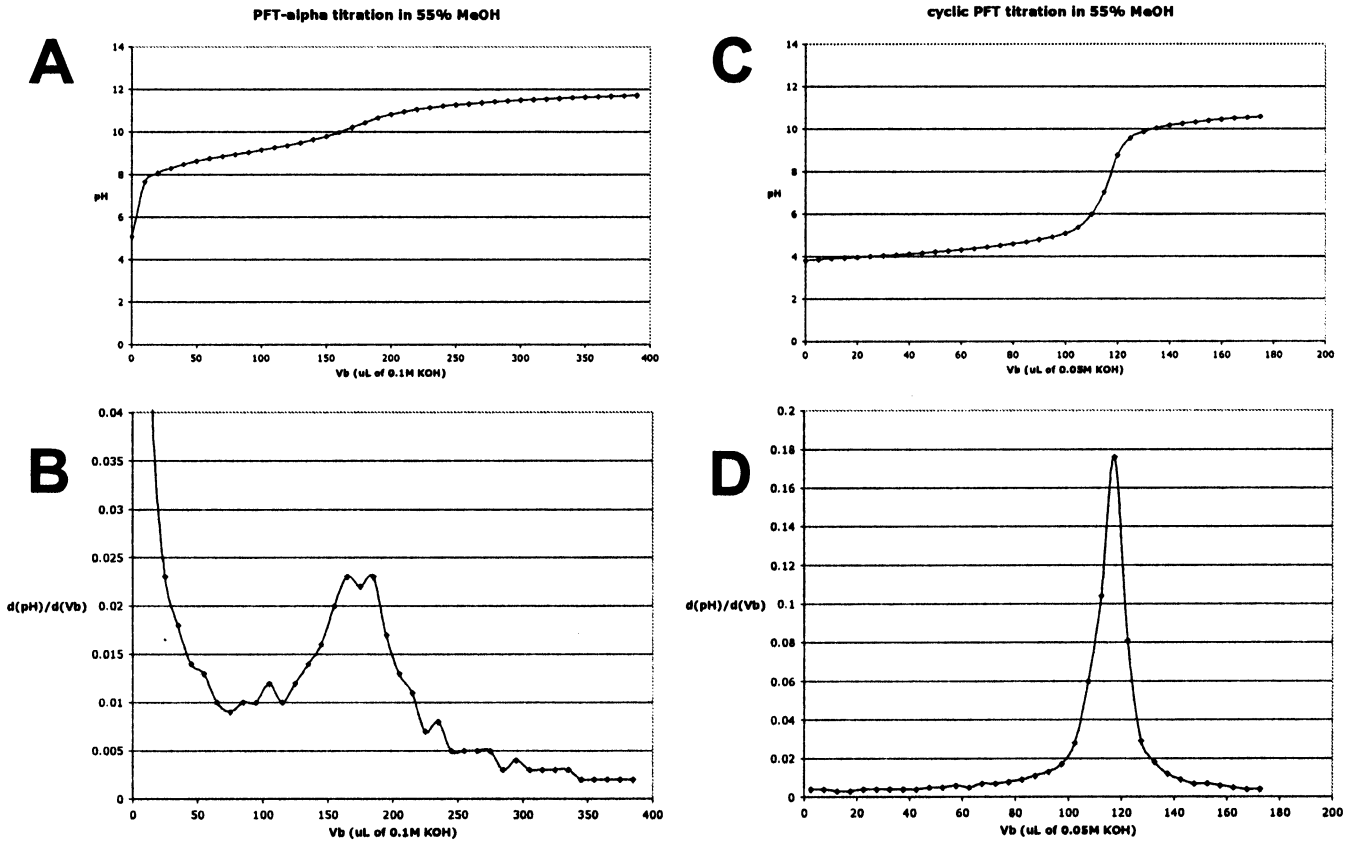

Figure 6. Titrations near the solubility limit. A typical titration in methanol−water cosolvent is shown for each compound. (A) Titration of 2.53 mM PFT-α in 55% MeOH. (B) First derivative of PFT-α titration. (C) Titration of 0.74 mM cyclic-PFT in 55% MeOH. (D) First derivative of cyclic-PFT titration.

Table 1. Acid Dissociation Constants at 0.1 M Ionic Strength, 25 °C

	pK_a			
R (MeOH wt %)	pH_{obs}[a]	p_cH[b]	$pK_a + \log [H_2O]$	pK_a
		PFT-α		
60	9.000	8.724	10.015	
55	9.025	8.771	10.118	
50	9.070	8.838	10.236	
45	9.050	8.846	10.291	
0		(extrap)	10.850	9.11
		Tricyclic PFT		
70	4.150	3.852	5.462	
65	4.230	3.925	5.358	
60	4.265	3.947	5.243	
55	4.305	4.010	5.153	
50	4.340	4.064	5.009	
0		(extrap)	6.109	4.36

[a] To nearest 0.005. [b] Calculated using four-parameter equation for methanol−water electrode calibration.

values to obtain the pK_a of each compound in the absence of methanol. PFT-α has a pK_a of 9.11, and cyclic-PFT has a pK_a of 4.36 (Table 1). Therefore, at pH 7, PFT-α is a positively charged species (>99% protonated), whereas its cyclic derivative is neutral (>99% unprotonated). These results explain the dramatic difference in solubility of these two compounds under physiological conditions. When PFT-α converts to its tricyclic derivative, the transformation produces a very weak base, nearly 5 orders of magnitude weaker than the parent compound.

Characterization of the Tricyclic Derivative: log *P*. The logarithm of the octanol−water partition coefficient, log *P*, is the most popular measure of lipophilicity used in pharmaceutics. The value of log *P* can be determined from analyte behavior during reversed-phase HPLC.[19,20] Log capacity factor (k') was plotted versus the volume fraction of methanol in the mobile phase (φ) for the tricyclic PFT derivative and four *n*-alkylbenzene standards having known log *P* values (Figure 8). Extrapolating these plots to $\varphi = 0$ gives the chromatographic parameter k'_w (Table 2), which best correlates with experimentally determined octanol−water partition coefficients. The observed k'_w values for the standards were plotted against their log octanol−water partition coefficients taken from the literature[21] (Figure 9), and this relationship was used to find log *P* of cyclic-PFT

(19) Harnisch, M.; Möckel, H. J.; Schulze, G. Relationship between log Pow shake-flask values and capacity factors derived from reversed-phase high-performance liquid chromatography for *n*-alkylbenzenes and some OECD reference substances. *J. Chromatogr.* **1983**, *282*, 315−332.

(20) Braumann, T. Determination of hydrophobic parameters by reversed-phase liquid chromatography: theory, experimental techniques, and application in studies on quantitative structure-activity relationships. *J. Chromatogr.* **1986**, *373*, 191−225.

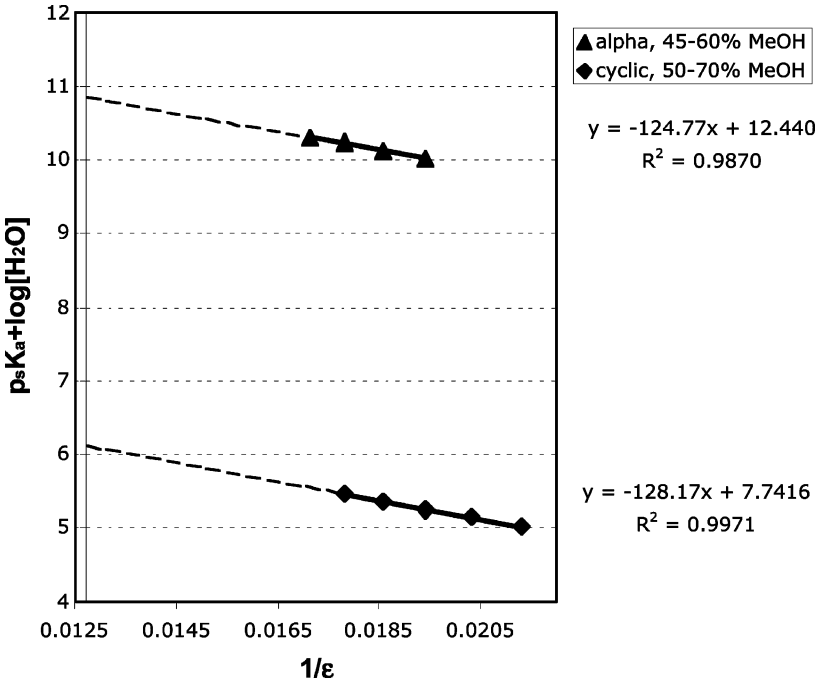

Figure 7. Yasuda−Shedlovsky extrapolation for titrations in methanol−water. A linear relationship exists between the inverse of the cosolvent dielectric constant and the sum of the apparent pK_a and log [H_2O]. Data for PFT-α in 45−60% (w/w) MeOH (triangles) and cyclic-PFT in 50−70% (w/w) MeOH (diamonds) are extrapolated to 0.01274, the reciprocal of the dielectric constant of water.

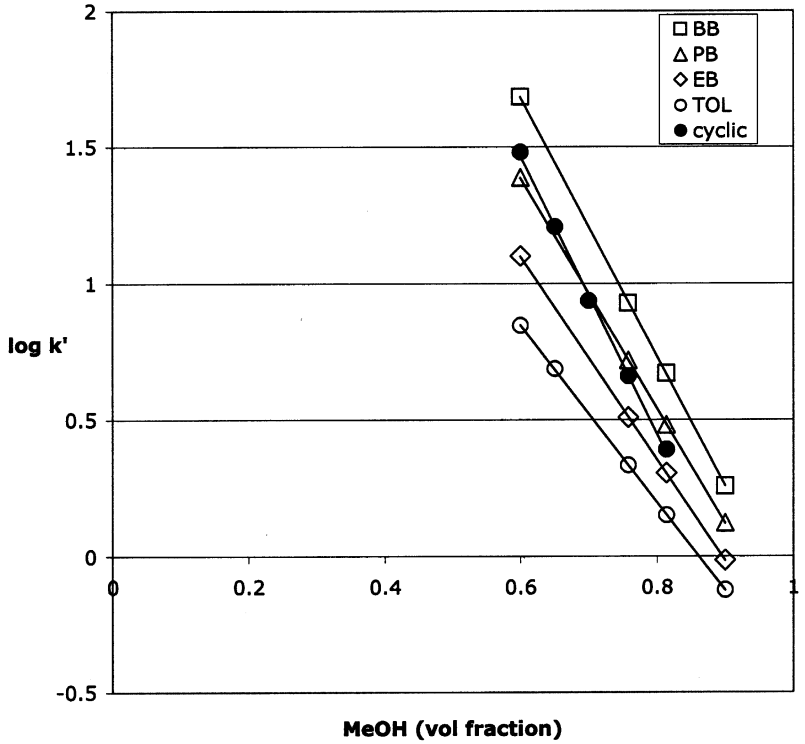

Figure 8. Determination of log k'_w for cyclic-PFT (filled circles) and *n*-alkylbenzene standards (open symbols) by HPLC.

= 4.26. This experimental value was in close agreement with the calculated log *P* of 4.15 predicted by the ChemSilico neural network QSAR model (ChemSilico, Tewksbury, MA; www.chemsilico.com). Several other log *P* predictor algorithms were less successful in matching the experimental result. Because PFT-α is strongly basic, measurement of its log *P* by a parallel experimental procedure would necessitate either an unacceptably high mobile phase pH or modification of the procedure to incorporate ionization corrections. Instead, because the experimental result for cyclic-PFT appeared to validate the use of the ChemSilico algorithm for this family of compounds, this prediction method was

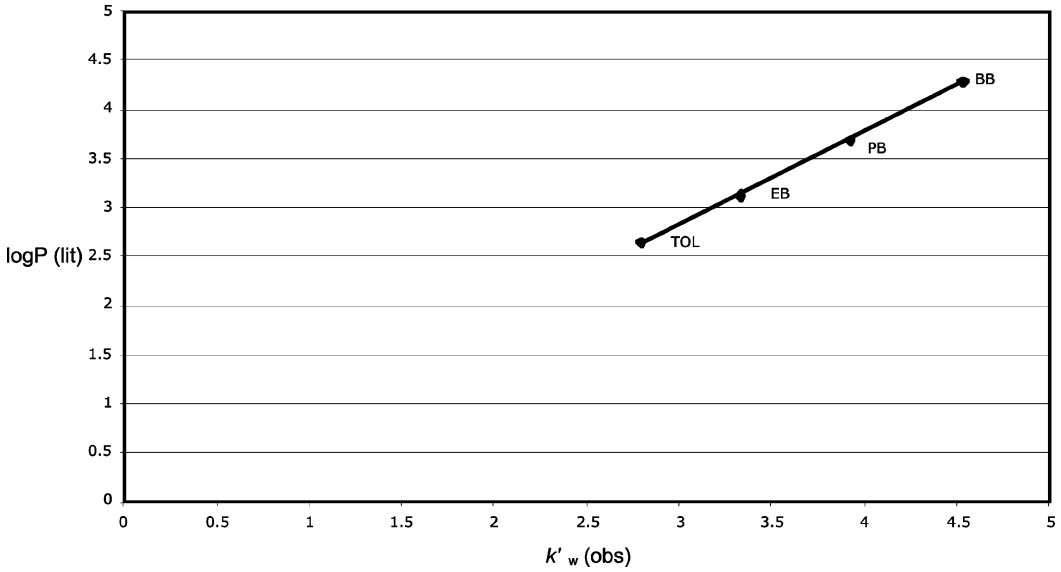

Figure 9. Standard curve for log *P* versus experimental k'_w values. TOL = toluene, EB = ethylbenzene, PB = *n*-propylbenzene, BB = *n*-butylbenzene.

Table 2. HPLC Capacity Factor at Zero Organic Modifier (k'_w) and log *P*

compound	φ vs log k' regression (R^2)	log k'_w	log *P*	log *P* method
toluene	1.0000	2.7925	2.65	oct−water, ref 21
ethylbenzene	1.0000	3.3304	3.13	oct−water, ref 21
n-propylbenzene	1.0000	3.9226	3.69	oct−water, ref 21
n-butylbenzene	1.0000	4.5331	4.29	oct−water, ref 21
cyclic-PFT	0.9989	4.5166	4.26	HPLC, this study
PFT-α	nd[a]	nd	2.24	calculated

[a] Not determined.

selected as the most accurate for PFT-α estimation. In this way, a calculated log *P* of 2.24 was obtained for PFT-α.

Characterization of the Tricyclic Derivative: Aqueous Solubility. The aqueous solubility of cyclic-PFT was measured by comparing the absorbance of a saturated solution in water to a standard curve. First, the absorbance of cyclic-PFT in methanol solution was recorded (Figure 10, upper panel). The protonated species of cyclic-PFT (pH 3 and lower) had an absorbance maximum at 250.5 nm and a molar extinction coefficient at this wavelength of 28 700 M^{-1} cm^{-1}. The unprotonated form of cyclic-PFT (pH 6 and higher) had an absorbance maximum at 260.0 nm and a molar extinction coefficient at this wavelength of 26 100 M^{-1} cm^{-1}. The aqueous solubility was measured several times, with a typical experiment shown (Figure 10, lower panel). Cyclic-PFT in methanol solution was added to PBS at pH 7.0 to give a final concentration of 43 μM, and the mixture became milky immediately. The saturated suspension was agitated continuously for 24 h; then it was passed through a 0.45 μm filter to remove insoluble precipitate, and absorbance scans of the filtrate were recorded. For comparison, a parallel experiment was conducted in which 43 μM cyclic-PFT was added to PBS that had been adjusted to pH 2.9 with HCl in order to evaluate the behavior of the soluble, protonated form. The acidified aqueous solution yielded an absorbance spectrum identical to that observed for the protonated species in methanol (Figure 10, blue curves of upper and lower panels). Filtration had very little effect on the absorbance of the soluble species (Figure 10, lower panel, blue and pink curves). In contrast, the saturated suspension in pH 7 PBS showed low apparent absorbance at all wavelengths, indicative of light scattering by fine particles; after filtration, only slight absorbance was evident (Figure 10, lower panel, green and orange curves). After correction for traces of UV-absorbing material originating from the filter, the concentration of the saturated aqueous solution was found to be 0.2 μM. The initial milky suspension was highly scattering, but it gradually clarified during the 24 h incubation period due to the tendency of the insoluble particulate to aggregate and adhere to the walls of the tube. UV absorbance was quantitatively recovered by emptying of the tube and redissolving of the adherent material with methanol (data not shown).

Structural Comparison of PFT-α and Its Tricyclic Derivative. Given the rapid conversion of PFT-α to its tricyclic derivative, it seems likely that most studies involving PFT-α have used mixed compositions of PFT-α and compound **2**. The structural differences between the two molecules are quite significant, as shown by comparison of the energy-minimized conformations of each (Figure 11). The tetrahydrobenzothiazoline rings of PFT-α can be superimposed on the tricyclic derivative, but beyond this common region the two structures diverge considerably. The atoms are colored as C = green, S = yellow, N = blue, O = red, and H = white, and the portion of cyclic-PFT that cannot be superimposed with PFT-α is shown in magenta. The full

(21) Schantz, M. M.; Martire, D. E. Determination of hydrocarbon-water partition coefficients from chromatographic data and based on solution thermodynamics and theory. *J. Chromatogr.* **1987**, *391*, 35−51.

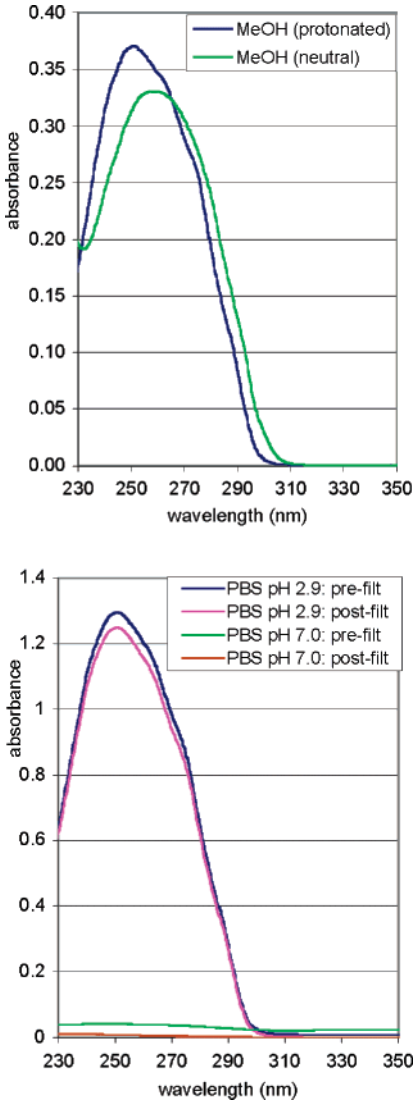

Figure 10. Aqueous solubility of cyclic-PFT. Absorbance scans of cyclic-PFT in methanol at low and high pH (upper panel). Absorbance scans of cyclic-PFT in buffered water at low and high pH before and after 0.45 μm filtration (lower panel).

face view displays the central tetrahedral carbon that is specific to PFT-α, whereas the edge view emphasizes the highly planar geometry of the tricyclic derivative. PFT-α is shown as the protonated imine form. The sp^3 hybridized carbon that is α to the ketone causes the *p*-tolyl portion of PFT-α to project out of the plane defined by its tetrahydrobenzothiazoline rings by an angle of 94°, whereas the *p*-tolyl extension is coplanar in cyclic-PFT. Cyclization causes subtle structural changes in the thiazole portion of the molecule. The carbon−nitrogen bond that is common to the fused thiazole and imidazole rings in compound **2** exhibits considerable double bond character, with a calculated bond length of 1.37 Å in the tricyclic compound and 1.45 Å for the corresponding bond length in PFT-α. Most significantly, the imine group of PFT-α carries a formal charge of +1 at physiological pH, whereas compound **2** is uncharged. In its interactions with potential cellular targets, this region of

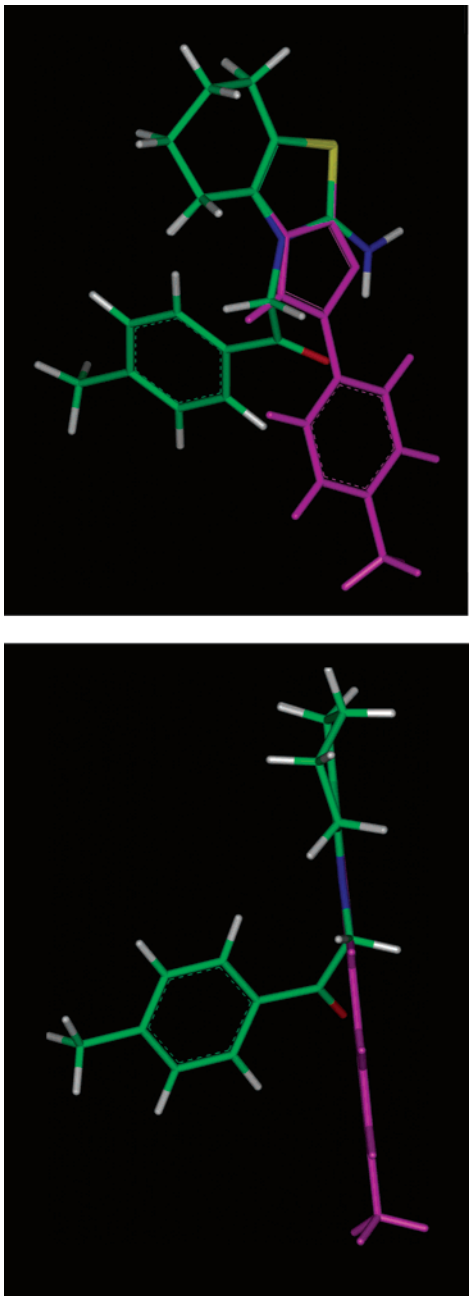

Figure 11. Two views of superimposed PFT-α and cyclic-PFT structures. Portions of cyclic-PFT that cannot be superimposed are colored in magenta.

PFT-α might participate in salt bridges or other electrostatic associations that would not be available to the planar tricyclic derivative.

Intramolecular Cyclization Converts PFT-α to Its Tricyclic Derivative. A proposed reaction mechanism for the conversion of PFT-α to its tricyclic derivative via intramolecular cyclization is shown (Scheme 1). One prediction of this mechanism is that the ketone function in PFT-α is required for its degradation. To test this prediction, we made an analogue of PFT-α that lacks the carbonyl moiety and tested its stability with respect to chromatographic behavior and formation of insoluble precipitate. This analogue (compound **3**) failed to generate insoluble products at

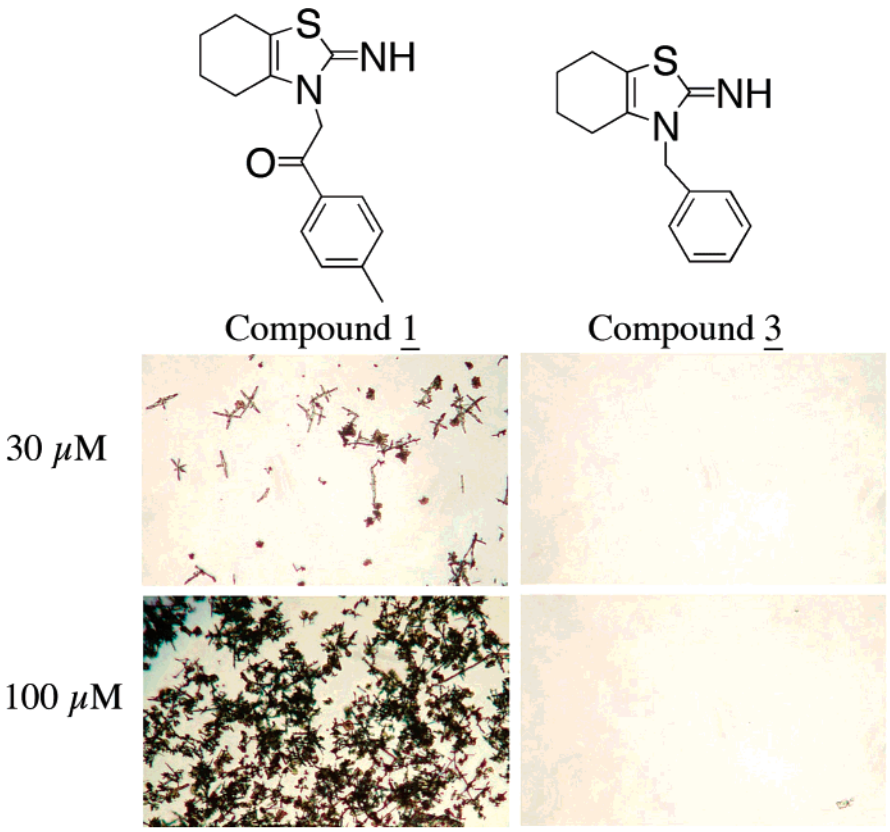

Figure 12. Compound **3**, a PFT analogue that is incapable of cyclization, is stable and does not form an insoluble precipitate.

Scheme 1

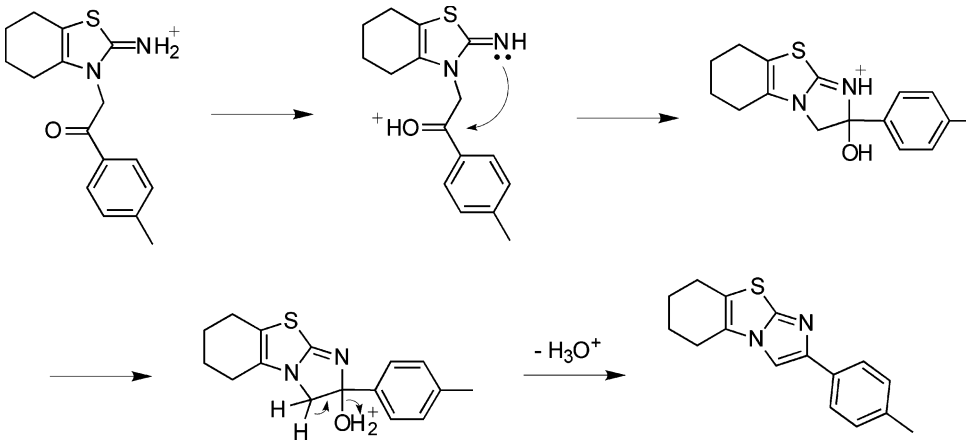

any concentration (Figure 12). In contrast, PFT-α produced copious precipitate in a time- and temperature-dependent manner, as expected. Compound **3** had an HPLC retention time similar to that of PFT-α, but HPLC revealed no signs of degradation of compound **3** after 48 h at 37 °C (data not shown). The stability of compound **3** proves that intramolecular cyclization is the process that is involved in the spontaneous degradation of PFT-α, and not another chemical process such as oxidation or hydrolytic deamination which might have been mistakenly identified as cyclization. In conjunction with the NMR data, these results provide unequivocal identification of compound **2** as the correct structure of the PFT-α degradation product.

Discussion

As PFT-α undergoes spontaneous conversion to its tricyclic derivative, the drug becomes insoluble and precipitates from solution, unless high concentrations of albumin or other lipophilic carrier are present to sequester the product. The precipitate can assume various morphologies depending on conditions of crystal growth, with long branched crystalline fibers representing a common form when cyclic-PFT is produced gradually from the parent compound. In aqueous media, cyclic-PFT tends to adhere to the walls of its container as a thin film that cannot be dislodged by vortexing. PFT-α has a pK_a of 9.11 and is therefore fully protonated at pH 7.

As an ionic species, its aqueous solubility is not a limiting factor in its use as a pharmacological agent. However, cyclic-PFT has a pK_a of 4.36 and is therefore uncharged at pH 7. Scheme 1 shows the loss of the charge-carrying proton plus one water molecule during the cyclization reaction that generates cyclic-PFT. As indicated by its log *P* of 4.26, cyclic-PFT is a very hydrophobic molecule. The log *P* of PFT-α is approximately 2 log units less than that of cyclic-PFT, so even with respect to their neutral forms, the two molecules are markedly different in this regard. The higher log *P* of the cyclic derivative can be understood by inspection of the structures of the neutral species of the molecules; the two most polar features of PFT-α, the ketone and the exocyclic imine, are absent in cyclic-PFT. The strikingly different chromatographic behaviors of these compounds during reversed-phase HPLC (Figure 3) can be explained by differences in ionization (as reflected by pK_a) and intrinsic hydrophobicity (as reflected by log *P*). These same factors account for the dramatic differences in aqueous solubility.

The aqueous solubility of cyclic-PFT was found to be 0.2 μM. The equilibrium between solubilization and precipitation is determined mainly by hydrophobicity, which can be expressed as the preference of a molecule for the octanol phase in an octanol−water partition experiment, and by the attractive intermolecular forces of the crystal lattice, which can be related to the melting point temperature needed to overcome this attraction. The general solubility equation for the aqueous solubility of an organic nonelectrolyte can be used to estimate solubility using these parameters as follows: $\log S_w = 0.5 - \log P - 0.01(\mathrm{mp} - 25)$, in which S_w is the aqueous solubility in mol L^{-1}, and mp is the melting point in °C.[22] Using this equation for cyclic-PFT with the melting point of 185 °C[11] and log *P* of 4.26 (Table 2), solubility is estimated to be 4 μM. This overestimate of aqueous solubility may reflect the shortcomings of the general solubility equation as a predictor in this instance. It is also possible that the experimental value for log *P* could be slightly low, considering that the goodness-of-fit observed during the extrapolation to k'_w, though excellent, was lower for cyclic-PFT as compared to the standards (Table 2). Better agreement between the experimental and calculated solubility was obtained using the WATERNT v1.01 program of the WaterFrag module of EPI Suite v3.12 from the U.S. Environmental Protection Agency. This is a structure-based prediction method that calculates the predicted aqueous solubility at 25 °C by summing solubility coefficients from atom/fragment contributions. The estimated solubility of cyclic-PFT by this method is 0.9 μM.

The precise mechanism of action of PFT-α is unknown. It has not been reported to bind directly to the p53 protein, so it might act within any of the pathways that functionally interact with p53. If one seeks to understand the molecular basis for PFT-α activity, the structural features of the pharmacophore are important for guidance. At present, it is unclear whether the pharmacological effects of PFT-α are due to the interaction of the parent molecule with its molecular targets, the interaction of the tricyclic degradation product with its molecular targets, or some combination of both. On the basis of the results presented here, the transport properties and intracellular compartmentalization of PFT-α and its tricyclic derivative could be expected to be quite different. In terms of hydrophobicity, PFT-α represents a fairly typical drug, whereas cyclic-PFT would rank among the more hydrophobic. The average log *P* for compounds listed in the Comprehensive Medicinal Chemistry database is 2.52.[23] As a point of reference for interpreting log *P* values, one of Lipinski's rule-of-five criteria for predicting oral bioavailability is that log *P* be less than 5.[24,25] It seems likely that cyclic-PFT would accumulate in biological membranes of treated cells. p53 is a soluble protein that is synthesized in the cytoplasm and transported to its site of action in the nucleus, where it can bind to DNA and interact with transcriptional machinery. The import and export of p53 into and out of the nucleus is one mechanism by which p53 function is regulated.[26] Conceivably, accumulation of cyclic-PFT within the nuclear membrane could in some way affect nuclear import of p53. PFT-α has been reported to increase the functional nuclear pore size in translocation studies using mouse fibroblasts.[27] A second study specifically examining the nuclear translocation of p53 after treatment with PFT-α found no effect of the drug,[8] although cells were treated for only 2 h in this assay, so formation of cyclic-PFT was not as great as it would be in most experiments. With greater awareness that PFT-α converts to a highly hydrophobic product, future experiments may be designed with the possibility of a membrane site of action in mind.

The pK_a measurements establish that PFT-α is protonated at neutral pH. In Scheme 1, we represent the imine of PFT-α as the site of protonation, on the basis of our NMR results. This is consistent with prior studies that have found that the exocyclic nitrogen is the site of protonation for both 3-methyl-2-iminothiazoline and 3-methyl-2-iminobenzothiazoline.[28] These compounds have pK_a's of 9.50 and 7.96,

(22) Jain, N.; Yalkowsky, S. H. Estimation of the aqueous solubility I: Application to organic nonelectrolytes. *J. Pharm. Sci.* **2001**, *90*, 234−252.

(23) Darvas, F.; Keseru, G.; Papp, A.; Dorman, G.; Urge, L.; Krajcsi, P. In silico and ex silico ADME approaches for drug discovery. *Curr. Top. Med. Chem.* **2002**, *2*, 1287−1304.

(24) Lipinski, C. A.; Lombardo, F.; Dominy, B. W.; Feeney, P. J. Experimental and computational approaches to estimate solubility and permeability in drug discovery and development settings. *Adv. Drug Delivery Rev.* **1997**, *23*, 3−25.

(25) Lipinski, C. A. Lead- and drug-like compounds: the rule-of-five revolution. *Drug Discovery Today: Technol.* **2004**, *1*, 337−341.

(26) O'Brate, A.; Giannakakou, P. The importance of p53 location: nuclear or cytoplasmic zip code? *Drug Resist. Updates* **2003**, *6*, 313−322.

(27) Feldherr, C. M.; Akin, D.; Cohen, R. J. Regulation of functional nuclear pore size in fibroblasts. *J. Cell Sci.* **2001**, *114*, 4621−4627.

(28) Forlani, L.; De Maria, P. Tautomerism of aminothiazoles. pK_{BH+} values of 2-aminothiazoles and some model imines. *J. Chem. Soc., Perkin Trans. 2* **1982**, 535−537.

respectively.[28] At 9.11, the pK_a of PFT-α was intermediate between these two. In Scheme 1, it is proposed that a proton migration step occurs that would activate the imine as a nucleophile and the carbonyl as an electrophile. It is likely that such proton migration would be facilitated in a protic solvent, which would explain the kinetic differences observed for the reaction in water versus DMSO (Figure 5). The essential role of the carbonyl as the target of nucleophilic attack, shown in the next step, was confirmed experimentally by synthesizing the PFT-α analogue lacking carbonyl function (compound **3**) and observing that it was stable in terms of solubility and chromatographic behavior. Compound **3** is the only analogue of PFT-α lacking the ketone that has been described thus far. It was originally made as one of a large series of analogues that were characterized for biological activity,[10] but at that time the authors may not have recognized the special chemistry of this member of the series, as stability and potential for cyclization were not discussed. The final two steps of Scheme 1 involve proton migration and an elimination reaction, such that water and a proton depart in a coordinated manner to leave cyclic-PFT in its expected free base form.

The significant differences between PFT-α and its planar tricyclic derivative raise questions about the structural requirements of the pharmacophore in this family of inhibitors. The main structural feature shared by the parent compound and its cyclization product is the tetrahydrobenzothiazoline group. However, 2-amino-4,5,6,7-tetrahydrobenzothiazole is inactive,[10] indicating that N-substitution of the thiazole is necessary for activity. The conformational space accessible to the N-substituent chain is very different in the tetrahedral parent and its planar tricyclic derivative. For example, in the superimposed models of PFT-α and cyclic-PFT (Figure 11), the carbon atom of the *p*-methyl substituent on the phenyl ring of PFT-α is 8.47 Å distant from the same carbon in cyclic-PFT. If the tetrahydrobenzothiazoline and *p*-tolyl moieties are both important components of the pharmacophore, it seems that the molecular target of drug action would have a significant preference for one molecule or the other. Conversely, if the hybridization of the exocyclic nitrogen atom is a critical structural determinant, it is possible that the N-substituent could serve mainly to stabilize the imino form of the imino−amino tautomer that could otherwise exist in PFT-α. In the inactive 2-amino-4,5,6,7-tetrahydrobenzothiazole, the amino tautomeric form is the most stable.

It will be challenging to determine how much of PFT-α's activity is attributable to the parent molecule, and how much is due to the cyclic derivative, because even the purest preparations of PFT-α will begin to degrade during a typical experiment. The most commonly used assays of PFT-α activity employ as an end point the change in the survival of cells exposed to DNA-damaging drugs, a procedure which takes several days. Reporter-based assays that monitor gene expression from a p53-responsive promoter can be done more quickly, but still require a period that is lengthy relative to the aqueous half-life of PFT-α. It appears that both cyclic and noncyclic analogues of PFT-α possess biological activity. Another group working independently has recently reported the ability of PFT-α to cyclize, and they synthesized a novel cyclic analogue that surpasses PFT-α in potency in a neuronal cell survival assay.[13] The biological activity of compound **2** was not reported, but the newly described cyclic analogue is identical to compound **2** except that a nitro substituent replaces the methyl group on the phenyl ring. This group did not examine any analogues that are incapable of intramolecular cyclization, but we have shown that compound **3** is incapable of cyclization, and this compound is only one-half log unit less potent than PFT-α as measured by EC_{50} in the PC12 cell protection assay.[10] Thus, on the basis of the limited information currently available, it appears that both tricyclic and noncyclizable analogues of PFT-α may be active. Future work should be designed with the potential for cyclization in mind. New analogues can be designed to be either cyclized (e.g., compound **2**), cyclogenic (e.g., compound **1**), or incapable of cyclization (e.g., compound **3**). Additional studies will be needed to discern which type of analogue has greatest utility. Disregarding issues of potency and efficacy, analogues incapable of cyclization would probably be most attractive from a pharmaceutics perspective. The tricyclic derivative of PFT-α is very hydrophobic and a very weak base, giving it the undesirable tendency to precipitate from aqueous solution. Cyclogenic drugs such as PFT-α have an additional drawback in that they are intrinsically unstable, complicating the handling of the drug and the interpretation of its effects. Because PFT-α was identified from a chemical library by random screening, it probably does not represent a pharmaceutically optimized compound. Cognizance of the intramolecular cyclization reaction and its physicochemical consequences can guide the rational design of new p53 inhibitors that are stable and remain soluble indefinitely.

Acknowledgment. We thank Dr. Pradip Bhowmik, Dr. Lydia McKinstry, and Dr. David Emerson for helpful discussions. This work was supported by an NIH/BRIN Faculty Development Initiative award (to R.K.G.), an Applied Research Initiative grant from Cosmepure, Intl./CellMedics, Ltd. (to R.K.G.), and the UNLV Office of Research and Graduate Studies.

MP050055D